


Write-error reduction in voltage-driven magnetization switching using a recording layer with low magnetic damping

Tatsuya Yamamoto¹,* Tomohiro Ichinose, Takayuki Nozaki, Shingo Tamaru, Kay Yakushiji², Hitoshi Kubota², and Shinji Yuasa

National Institute of Advanced Industrial Science and Technology (AIST), Research Center for Emerging Computing Technologies, Tsukuba, Ibaraki 305-8568, Japan

 (Received 8 January 2024; revised 8 April 2024; accepted 15 April 2024; published 3 May 2024)

We develop perpendicularly magnetized magnetic tunnel junctions consisting of a recording layer exhibiting a low magnetic damping to investigate the influence of magnetic damping on the write-error rate of voltage-driven magnetization switching. The effective magnetic damping is reduced to about one-third that of a conventional Ta/Co-Fe-B/MgO recording layer by eliminating the spin pumping effect. The low magnetic damping contributes to a 3-orders-of-magnitude reduction in the write-error rate for the longer write pulses, which is explained by the suppression of thermal fluctuation during the switching process. The low magnetic damping also enables a long period of magnetization precession to control the dynamics via the voltage-controlled magnetic anisotropy effect.

DOI: [10.1103/PhysRevApplied.21.054008](https://doi.org/10.1103/PhysRevApplied.21.054008)

I. INTRODUCTION

Voltage-controlled magnetic anisotropy (VCMA) offers energy-efficient ways of manipulating magnetization in magnetic thin films [1–8]. In particular, the use of VCMA in Co-Fe alloys/MgO junctions is a promising solution for reducing the write energy of the magnetic memory cell in magnetoresistive random access memory (MRAM) [9–13]. Magnetic tunnel junctions (MTJs) using a Co-Fe alloys/MgO junction exhibit a large tunneling magnetoresistance (TMR) [14–16] as well as a perpendicular magnetic anisotropy (PMA) [17–20] and are compatible with state-of-the-art MRAM driven by the spin-transfer torque (STT) [9–13]. The VCMA effect in Co-Fe alloys/MgO junctions can be explained in terms of selective electron or hole doping in the d -electron orbitals [2,5,7] and/or the induction of magnetic dipole moment [21], and both of these mechanisms enable electrical control of the sub-nanosecond dynamics of magnetization in Co-Fe thin films, as demonstrated by the excitation of ferromagnetic resonance (FMR) [22–25] and parametric resonance by the application of microwave electric fields [26–28]. Moreover, the experimental demonstration of magnetization switching by voltage pulses [29,30] presents a basic idea for achieving VC-MRAMs.

The write process in VC-MRAM is quite different from that of STT-MRAM. Specifically, while both MRAMs consist of memory cells made of MTJs with a recording layer whose magnetization direction can be controlled

by an external electric signal, the write process in the VC-MRAM is mediated by the ultrafast on-off control of PMA in the recording layer. During the application of write voltage, the recording layer magnetization undergoes precessional motion around the effective field, and a controlled switching of magnetization can be achieved by turning off the voltage after an adequate duration [29–31]. Unlike in the case of STT-MRAM, the polarity of the recording layer in VC-MRAM cannot be uniquely determined by switching the polarity of the write voltage, and a precise control of write pulse shape is necessary to reduce the write-error rate (WER) [32].

For reducing the WER in VC-MRAM, it is also important to deal with the thermal fluctuation. At a finite temperature T , the thermal noise randomly fluctuates the orbital motion of magnetization, and the WER cannot be reduced to zero even if the write pulse width (t_p) is set exactly equal to one-half of the precession period. There are several ways of reducing the effect of thermal fluctuation. One is to shorten t_p as the magnetization is most sensitive to the thermal noise when the PMA is reduced to zero by the application of write voltage. Since the optimum t_p for minimizing WER is determined by the resonance frequency of the recording layer magnetization, a shorter t_p can be achieved by increasing the external field along the precession axis. In fact, WERs lower than 10^{-6} have been demonstrated for t_p as short as 0.2 ns [33]. Although a shorter write time is also beneficial in terms of energy efficiency, the use of extremely short pulses is unacceptable for practical memory devices. Also, the external field necessary to reduce the WER should be as small as possible

*Corresponding author: yamamoto-t@aist.go.jp

to avoid the complexity of the MTJ stack and/or the device design.

Another strategy to reduce the WER is to use a recording layer with a low damping constant (α). By assuming a Gaussian distribution, the random field h due to the thermal noise possesses statistical properties defined by [34]

$$\langle h_i(t) \rangle = 0, \langle h_i(t) h_j(t') \rangle = 2D \delta_{ij} \delta(t - t'), \quad (1)$$

where i and j are the Cartesian indices and D represents the strength of the thermal fluctuation, given by

$$D = \frac{\alpha}{1 + \alpha^2} \frac{k_B T}{\gamma M_s}, \quad (2)$$

where k_B is the Boltzmann constant, γ is the gyromagnetic ratio, and M_s is the saturation magnetization. Thus, for typical ferromagnets with $0 < \alpha < 0.1$, the lowering of α is as effective as the lowering of T for reducing the thermal fluctuation. Although Co-Fe alloys are known to exhibit ultralow intrinsic α [35], extrinsic contributions such as the spin pumping effect [36,37] enhance the effective damping α_{eff} . This enhancement of α_{eff} can be quite serious for VC-MRAM in which the recording layer is made of an ultrathin (approximately 1 nm) ferromagnetic layer since the α_{eff} enhancement due to the spin pumping effect is inversely proportional to the thickness of the ferromagnetic layer [35,37,38]. In fact, Ta/Co-Fe-B/MgO multilayers have most commonly been used in VCMA studies owing to their reasonably large PMA and VCMA efficiency despite the non-negligible spin pumping from the Co-Fe-B layer to the Ta layer. Although improved PMA and VCMA efficiencies have been demonstrated by a number of studies [25,39–50], it remains difficult to eliminate the spin pumping effect as long as a metallic layer is used as a counter electrode [51].

In this work, we develop MTJs consisting of a Co-Fe-B recording layer sandwiched by an $\text{Mg}_{40}\text{Fe}_{10}\text{O}_{50}$ (Mg-Fe-O) layer and an MgO layer. The nonmagnetic insulators on both sides of the Co-Fe-B recording layer effectively eliminate the spin pumping effect, and a low α_{eff} of 0.01 is achieved for a 1.4-nm-thick Co-Fe-B layer. The perpendicularly magnetized MTJs exhibit a large TMR ratio of over 200% as well as a sizable VCMA after annealing at 673 K. Owing to the low α_{eff} , the MTJs exhibit a fairly low WER of the order of 10^{-3} for $t_p > 1$ ns, and the external field necessary to achieve a minimum WER is reduced by half compared with conventional VCMA MTJs consisting of a Ta/Co-Fe-B/MgO multilayer [43,52].

II. EXPERIMENT

Figure 1 shows a schematic illustration of the MTJ as well as the measurement circuit used for the WER measurement. The MTJ consists of a Co-Fe-B(0.8 nm)/Mg-Fe-O(2.0 nm)/Co-Fe-B(1.4 nm)/Mo(0.3 nm)/

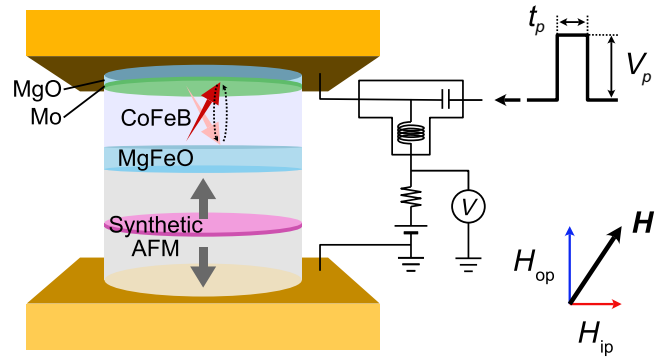


FIG. 1. Schematic illustration of the MTJ along with the measurement circuit used for WER measurement. The MTJ consists of a Co-Fe-B(0.8 nm)/Mg-Fe-O(2.0 nm)/Co-Fe-B(1.4 nm)/Mo(0.3 nm)/MgO(0.8 nm) multilayer. A tilted magnetic field \mathbf{H} is applied to the MTJ device during the WER measurement.

MgO(0.8 nm) multilayer, where the top 1.4-nm-thick Co-Fe-B layer acts as a recording layer and the magnetization direction of the lower 0.8-nm-thick Co-Fe-B is fixed by an adjacent CoPt-based synthetic antiferromagnetic (AFM) layer. The use of Mg-Fe-O instead of MgO improves the wettability of the top Co-Fe-B layer, which improves the PMA while reducing α_{eff} [53]. The atomically thin Mo layer absorbs boron atoms from the Co-Fe-B layer to promote crystallization by postannealing. Although an enhanced VCMA efficiency is reported for Mo-capped Co-Fe-B recording layers [54], here we design the Mo layer to be as thin as possible to minimize α_{eff} . The multilayers are deposited on 300-mm Si substrates using a mass-production-compatible sputtering system manufactured by Tokyo Electron Ltd. (TEL-EXIM). Both the Mg-Fe-O and MgO layers are deposited by rf magnetron sputtering from sintered targets. The top Co-Fe-B layer is deposited at 100 K [55,56] from a $\text{Co}_{40}\text{Fe}_{40}\text{B}_{20}$ target, and the whole stack is *ex situ* annealed at 673 K for 1 h. FMR measurements of blanket MTJ films are carried out using our custom-made vector network analyzer FMR apparatus [57]. The MTJ films are patterned into circular nanopillars with a diameter of ≈ 60 nm by Ar-ion etching through resist patterns defined by electron-beam lithography.

During the WER measurements, a tilted magnetic field \mathbf{H} is applied to the MTJ device, where the in-plane component of \mathbf{H} (H_{ip}) defines the precession axis of magnetization during the switching process and the out-of-plane component (H_{op}) cancels the stray field from the bottom Co-Fe-B layer. Voltage pulses with various t_p are fed into the MTJ through the rf port of a bias tee, and the WER is calculated from 2×10^5 trials. The amplitude of pulse voltage V_p is set to approximately 1 V, which doubles at the MTJ due to the impedance mismatch between the pulse generator and the MTJ [58]. All measurements are carried out at room temperature.

III. RESULTS AND DISCUSSION

Figure 2(a) shows FMR spectra obtained from the blanket MTJ film consisting of the Mg-Fe-O/Co-Fe-B/Mo/MgO (hereafter, MgFeO-CoFeB MTJ) multilayer under the microwave field with a frequency f of 25 GHz. For comparison, FMR spectra obtained from a conventional VCMA MTJ film consisting of a Ta/Co-Fe-B(1.1 nm)/MgO multilayer as a recording layer (hereafter, Ta-CoFeB MTJ) [43,52] are shown in Fig. 2(b). The MgFeO-CoFeB MTJ exhibits a substantially larger FMR signal compared with Ta-CoFeB even though the thickness difference in Co-Fe-B (0.3 nm) is considered. The spectral linewidths $\mu_0\Delta H_{\text{op}}$ are 14 and 51 mT for the MgFeO-CoFeB and Ta-CoFeB MTJs, respectively. These results suggest a reduced magnetic dead layer as well as an improved magnetic uniformity in the MgFeO-CoFeB MTJ. The dependence of $\mu_0\Delta H_{\text{op}}$ on f is shown in Fig. 2(c). The linear relationship between $\mu_0\Delta H_{\text{op}}$ and f can be expressed as [35]

$$\mu_0\Delta H_{\text{op}} = \frac{2h\alpha_{\text{eff}}}{g\mu_B}f + \mu_0\Delta H_0, \quad (3)$$

where h is Planck's constant, g is the Landé g -factor, μ_B is the Bohr magneton, and ΔH_0 is the inhomogeneous

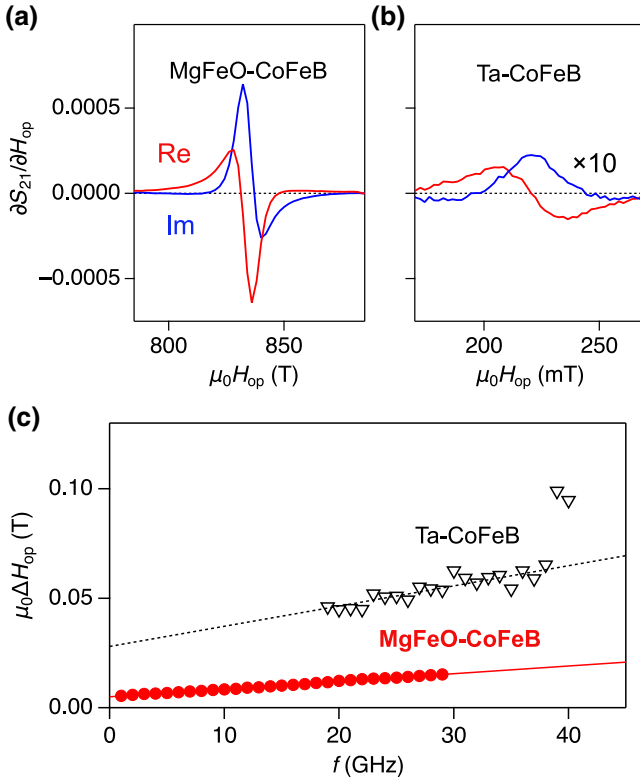


FIG. 2. FMR spectra obtained from the blanket MTJ films under H_{op} with $f = 25$ GHz. (a) MgFeO-CoFeB MTJ and (b) Ta-CoFeB MTJ. (c) FMR linewidth as a function of f . Lines denote fitting to the experimental data using Eq. (3).

linewidth. From the linear fitting to the experimental data using Eq. (3), we get $\alpha_{\text{eff}} = 0.011$ and $\mu_0\Delta H_0 = 5$ mT for the MgFeO-CoFeB MTJ, and $\alpha_{\text{eff}} = 0.028$ and $\mu_0\Delta H_0 = 28$ mT for the Ta-CoFeB MTJ. The reductions of α_{eff} and $\mu_0\Delta H_0$ in the MgFeO-CoFeB MTJ are attributed to the suppression of spin pumping effect and an improved magnetic homogeneity owing to the suppression of atomic diffusion, respectively.

Figure 3(a) shows magnetoresistance (R - H) curves obtained from the nanopillar MTJ device under an out-of-plane H . The device exhibits R - H curves typical for a perpendicularly magnetized MTJ, and the coercivity (H_c) changes on changing the bias voltage (V_{dc}). As shown in Fig. 3(b), H_c linearly changes with V_{dc} and the linear fitting to the experimental data (solid line) shows that H_c is reduced to zero by the application of $V_{\text{dc}} \approx 1.8$ V. Table I summarizes the values of TMR ratio, μ_0H_c ($V_{\text{dc}} = 0$), and $\mu_0\Delta H_c/\Delta V_{\text{dc}}$ [i.e., the y intercept and slope of the linear fitting shown in Fig. 3(b)] as well as the values of α_{eff} and $\mu_0\Delta H_0$ obtained from the FMR measurements. The MgFeO-CoFeB MTJ exhibits μ_0H_c and $\mu_0\Delta H_c/\Delta V_{\text{dc}}$ values similar to those of the Ta-CoFeB MTJ while substantial improvements in the TMR ratio, α_{eff} , and ΔH_0 are obtained.

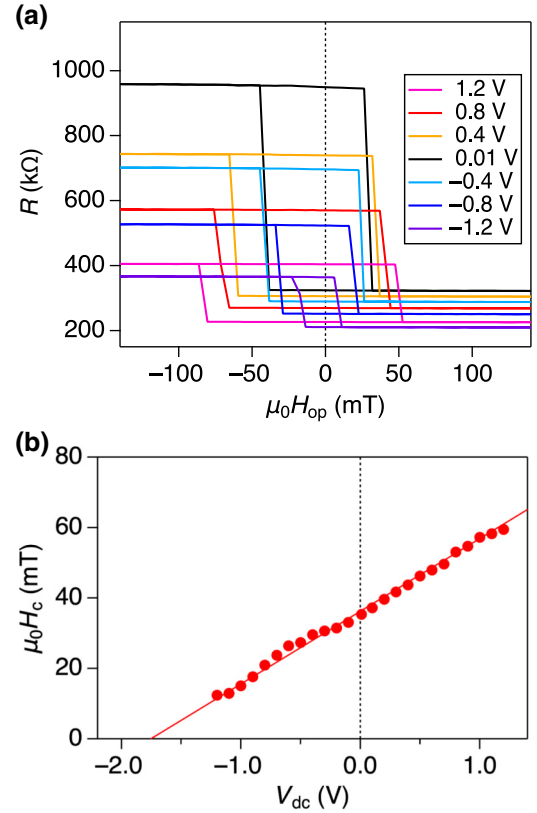


FIG. 3. (a) R - H curves measured under H_{op} with varying V_{dc} . (b) V_{dc} dependence of H_c . Solid line denotes the linear fitting to the experimental data.

TABLE I. Summary of magnetic and electrical transport properties of MTJs.

	α_{eff}	$\mu_0 \Delta H_0$	TMR ratio	$\mu_0 H_c (V_{\text{dc}} = 0)$	$\mu_0 \Delta H_c / \Delta V_{\text{dc}}$
MgFeO-CoFeB	0.011	5 mT	201%	36 mT	21 mT/V
Ta-CoFeB [43,52]	0.028	28 mT	77%	42 mT	18 mT/V

Figure 4(a) shows the WER measured under various H_{ip} . Here, H_{op} is kept constant at around 3 mT. The WER exhibits a clear minimum at a certain t_p corresponding to half of the magnetization precession period, and the position t_0 shifts in accordance with changing H_{ip} . Also, the dip structure broadens as H_{ip} is reduced, i.e., the controlled magnetization switching is achieved in a broader range of t_p for a lower H_{ip} . This is an important feature to mitigate the precision of pulse shape control required for switching the magnetization. The local maximum in WER observed for $t_p < t_0$ (e.g., $t_p = 0.22$ ns for $\mu_0 H_{\text{ip}} = 61.6$ mT) comes from the write error increase due to the thermally induced transition in the orbital motion of magnetization [52]. The precessional frequency (f_0) of magnetization during t_p can be calculated by using the relationship of $f_0 = 1/2t_0$ and is plotted as a function of H_{ip} in Fig. 4(b). The solid line in Fig. 4(b) denotes the Larmor frequency $f_L = \gamma \mu_0 H_{\text{ip}}$, where γ is the gyromagnetic ratio. For $\mu_0 H_{\text{ip}} > 30$ mT, f_0 almost agrees with f_L , which represents the uniform precession of magnetization along H_{ip} during the switching process. In contrast, the deviation of f_0 from f_L for $\mu_0 H_{\text{ip}} < 30$ mT suggests the presence of an

anisotropy field (e.g., magnetocrystalline anisotropy field) that inhibits uniform magnetization precession along H_{ip} .

The minimum value of WER is plotted as a function of H_{ip} in Fig. 4(c). For comparison, data obtained from the Ta-CoFeB MTJ [52] are also shown. While minimum WERs of the order of 10^{-4} are obtained for both MTJs, the H_{ip} dependencies are quantitatively different: for the MgFeO-CoFeB MTJ, the minimum WER is reduced to lower than 10^{-3} by the application of $\mu_0 H_{\text{ip}} > 30$ mT, whereas the Ta-CoFeB MTJ exhibits a minimum WER of the order of 10^{-1} for $\mu_0 H_{\text{ip}} \approx 40$ mT. This remarkable difference in the minimum WER for the low- H_{ip} region is attributed to the reduced thermal fluctuation owing to the low α_{eff} in the MgFeO-CoFeB MTJ. According to Eq. (2), the reduction in α_{eff} from 0.028 to 0.011 is equivalent to lowering T from 300 to 118 K in terms of D . Therefore, the MgFeO-CoFeB MTJ is more tolerant to increasing t_p (i.e., decreasing H_{ip}) while keeping a lower WER compared with the Ta-CoFeB MTJ. It should be noted that although the WER of the present MgFeO-CoFeB MTJ increases by the application of relatively small H_{ip} , the H_{ip} range as well as the WER itself will be readily improved by applying

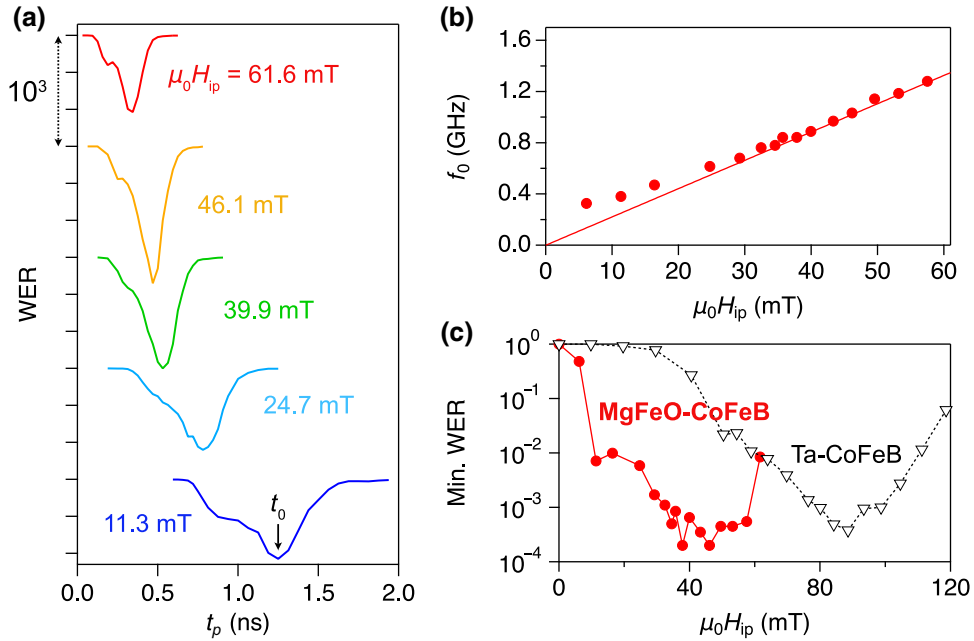


FIG. 4. (a) WER measured under various H_{ip} . Data are vertically offset for clarity. (b) H_{ip} dependence of f_0 estimated from t_0 . Solid line denote the Larmor frequency: $f_L = \gamma \mu_0 H_{\text{ip}}$. (c) H_{ip} dependence of minimum WER. Data denoted by the open symbols are from Ref. [52].

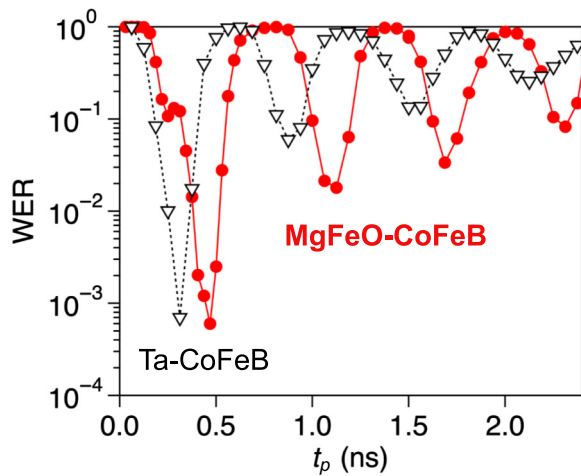


FIG. 5. Dependence of WER on t_p . Filled symbols: MgFeO-CoFeB MTJ under $\mu_0 H_{ip} = 46$ mT. Open symbols: Ta-CoFeB under $\mu_0 H_{ip} = 93$ mT.

a recording layer possessing a larger PMA and a larger VCMA efficiency.

The use of a low- α_{eff} recording layer is also beneficial for controlling the long-period precession of magnetization in MTJs. Figure 5 shows the periodic oscillation of WER obtained from the two MTJs. Here, $\mu_0 H_{ip} = 46$ mT for the MgFeO-CoFeB MTJ and $\mu_0 H_{ip} = 93$ mT for the Ta-CoFeB MTJ. The difference in the oscillation period is due to the difference in H_{ip} . Even though the MgFeO-CoFeB MTJ is disadvantageous in that the recording layer magnetization precesses at a lower frequency and thus suffers the thermal agitation field for a longer time at the same period of precession, it exhibits a lower WER for a longer period of oscillation compared with the Ta-CoFeB MTJ. For example, both MTJs exhibit almost the same WERs in the first period of oscillation, and in the second period, a difference of about 10 times appears. The MgFeO-CoFeB MTJ exhibits WER of the order of 10^{-2} even for the fourth period of WER oscillation, thus enabling the utilization of a long-term magnetization precession in the MTJ. The intrinsically small damping will also be beneficial for achieving VCMA-induced parametric resonance [26–28] for more precisely controlling the dynamics of magnetization.

IV. SUMMARY

To summarize, we investigate the influence of α_{eff} on the WER of magnetization switching driven by the VCMA effect. Perpendicularly magnetized recording layers exhibiting a low α_{eff} of 0.011 are fabricated by suppressing the spin pumping to the adjacent layers while maintaining a sizable VCMA effect. The low α_{eff} in the recording layer effectively reduces the thermal fluctuation during the switching process, which contributes to a

substantial improvement in the WER for the longer write pulses. The low α_{eff} also enables a persistent precession of magnetization in the recording layer, which will be useful to control the magnetization dynamics in the gigahertz range via the VCMA effect.

ACKNOWLEDGMENTS

The authors thank Y. Hibino, H. Imamura, S. Tsunegi, L. Sakai, K. Ohba, Y. Higo, Y. Kageyama, and M. Hosomi for fruitful discussions, and M. Toyoda for assisting with the experiments. This work is based on results obtained from projects JPNP16007 and JPNP20017 commissioned by the New Energy and Industrial Technology Development Organization (NEDO), Japan.

- [1] M. Weisheit, S. Fähler, A. Marty, Y. Souche, C. Poinsignon, and D. Givord, Electric field-induced modification of magnetism in thin-film ferromagnets, *Science* **315**, 349 (2007).
- [2] T. Maruyama, Y. Shiota, T. Nozaki, K. Ohta, N. Toda, M. Mizuguchi, A. A. Tulapurkar, T. Shinjo, M. Shiraishi, S. Mizukami, Y. Ando, and Y. Suzuki, Large voltage-induced magnetic anisotropy change in a few atomic layers of iron, *Nat. Nanotechnol.* **4**, 158 (2009).
- [3] C. G. Duan, J. P. Velez, R. F. Sabirianov, Z. Zhu, J. Chu, S. S. Jaswal, and E. Y. Tsymlal, Surface magnetoelectric effect in ferromagnetic metal films, *Phys. Rev. Lett.* **101**, 137201 (2008).
- [4] K. Nakamura, R. Shimabukuro, Y. Fujiwara, T. Akiyama, T. Ito, and A. J. Freeman, Giant modification of the magnetocrystalline anisotropy in transition-metal monolayers by an external electric field, *Phys. Rev. Lett.* **102**, 187201 (2009).
- [5] M. Tsujikawa and T. Oda, Finite electric field effects in the large perpendicular magnetic anisotropy surface Pt/Fe/Pt(001): A first-principles study, *Phys. Rev. Lett.* **102**, 247203 (2009).
- [6] T. Nozaki, Y. Shiota, M. Shiraishi, T. Shinjo, and Y. Suzuki, Voltage-induced perpendicular magnetic anisotropy change in magnetic tunnel junctions, *Appl. Phys. Lett.* **96**, 022506 (2010).
- [7] M. K. Niranjana, C.-G. Duan, S. S. Jaswal, and E. Y. Tsymlal, Electric field effect on magnetization at the Fe/MgO(001) interface, *Appl. Phys. Lett.* **96**, 222504 (2010).
- [8] Y. Shiota, S. Murakami, F. Bonell, T. Nozaki, T. Shinjo, and Y. Suzuki, Quantitative evaluation of voltage-induced magnetic anisotropy change by magnetoresistance measurement, *Appl. Phys. Express* **4**, 043005 (2011).
- [9] H. Yoda, *et al.*, High efficient spin transfer torque writing on perpendicularly magnetic tunnel junctions for high density MRAMs, *Curr. Appl. Phys.* **10**, e87 (2010).
- [10] D. C. Worledge, G. Hu, David W. Abraham, P. L. Trouiloud, and S. Brown, Development of perpendicularly magnetized Ta|CoFeB|MgO-based tunnel junctions at IBM, *J. Appl. Phys.* **115**, 172601 (2014).

- [11] K. Ando, S. Fujita, J. Ito, S. Yuasa, Y. Suzuki, Y. Nakatani, T. Miyazaki, and H. Yoda, Spin-transfer torque magnetoresistive random-access memory technologies for normally off computing, *J. Appl. Phys.* **115**, 172607 (2014).
- [12] L. Thomas, G. Jan, J. Zhu, H. Liu, Y.-J. Lee, S. Le, R.-Y. Tong, K. Pi, Y.-J. Wang, D. Shen, R. He, J. Haq, J. Teng, V. Lam, K. Huang, T. Zhong, T. Torng, and P.-K. Wang, Perpendicular spin transfer torque magnetic random access memories with high spin torque efficiency and thermal stability for embedded applications, *J. Appl. Phys.* **115**, 172615 (2014).
- [13] B. Dieny and M. Chshiev, Perpendicular magnetic anisotropy at transition metal/oxide interfaces and applications, *Rev. Mod. Phys.* **89**, 025008 (2017).
- [14] S. S. P. Parkin, C. Kaiser, A. Panchula, P. M. Rice, B. Hughes, M. Samant, and S.-H. Yang, Giant tunneling magnetoresistance at room temperature with MgO (100) tunnel barriers, *Nat. Mater.* **3**, 862 (2004).
- [15] S. Yuasa, T. Nagahama, A. Fukushima, Y. Suzuki, and K. Ando, Giant room-temperature magnetoresistance in single-crystal Fe/MgO/Fe magnetic tunnel junctions, *Nat. Mater.* **3**, 868 (2004).
- [16] D. D. Djayaprawira, K. Tsunekawa, M. Nagai, H. Maehara, S. Yamagata, N. Watanabe, S. Yuasa, Y. Suzuki, and K. Ando, 230% room-temperature magnetoresistance in CoFeB/MgO/CoFeB magnetic tunnel junctions, *Appl. Phys. Lett.* **86**, 092502 (2005).
- [17] T. Shinjo, S. Hine, and T. Takada, Mössbauer spectra of ultrathin Fe films coated by MgO, *J. de Phys.* **40**, C2 (1979).
- [18] S. Yakata, H. Kubota, Y. Suzuki, K. Yakushiji, A. Fukushima, S. Yuasa, and K. Ando, Influence of perpendicular magnetic anisotropy on spin-transfer switching current in CoFeB/MgO/CoFeB magnetic tunnel junctions, *J. Appl. Phys.* **105**, 07D131 (2009).
- [19] S. Ikeda, K. Miura, H. Yamamoto, K. Mizunuma, H. D. Gan, M. Endo, S. Kanai, J. Hayakawa, F. Matsukura, and H. Ohno, A perpendicular-anisotropy CoFeB-MgO magnetic tunnel junction, *Nat. Mater.* **9**, 721 (2010).
- [20] H. Kubota, S. Ishibashi, T. Saruya, T. Nozaki, A. Fukushima, K. Yakushiji, K. Ando, Y. Suzuki, and S. Yuasa, Enhancement of perpendicular magnetic anisotropy in FeB free layers using a thin MgO cap layer, *J. Appl. Phys.* **111**, 07C723 (2012).
- [21] M. Wang, W. Cai, K. Cao, J. Zhou, J. Wrona, S. Peng, H. J. Wei, W. Kang, Y. Zhang, J. Langer, B. Ocker, A. Fert, and W. Zhao, Current-induced magnetization switching in atom-thick tungsten engineered perpendicular magnetic tunnel junctions with large tunnel magnetoresistance, *Nat. Commun.* **9**, 671 (2018).
- [22] T. Nozaki, Y. Shiota, S. Miwa, S. Murakami, F. Bonell, S. Ishibashi, H. Kubota, K. Yakushiji, T. Saruya, A. Fukushima, S. Yuasa, T. Shinjo, and Y. Suzuki, Electric-field-induced ferromagnetic resonance excitation in an ultrathin ferromagnetic metal layer, *Nat. Phys.* **8**, 491 (2012).
- [23] J. Zhu, J. A. Katine, G. E. Rowlands, Y.-J. Chen, Z. Duan, J. G. Alzate, P. Upadhyaya, J. Langer, P. K. Amiri, K. L. Wang, and I. N. Krivorotov, Voltage-induced ferromagnetic resonance in magnetic tunnel junctions, *Phys. Rev. Lett.* **108**, 197203 (2012).
- [24] W. Skowroński, T. Nozaki, D. D. Lam, Y. Shiota, K. Yakushiji, H. Kubota, A. Fukushima, S. Yuasa, and Y. Suzuki, Underlayer material influence on electric-field controlled perpendicular magnetic anisotropy in CoFeB/MgO magnetic tunnel junctions, *Phys. Rev. B* **91**, 184410 (2015).
- [25] T. Nozaki, A.-K. Rachwał, M. Tsujikawa, Y. Shiota, X. Xu, T. Ohkubo, T. Tsukahara, S. Miwa, M. Suzuki, S. Tamaru, H. Kubota, A. Fukushima, K. Hono, M. Shirai, Y. Suzuki, and S. Yuasa, Highly efficient voltage control of spin and enhanced interfacial perpendicular magnetic anisotropy in iridium-doped Fe/MgO magnetic tunnel junctions, *NPG Asia Mater.* **9**, e451 (2017).
- [26] Y.-J. Chen, H. K. Lee, R. Verba, J. A. Katine, I. Barsukov, V. Tiberkevich, J. Q. Xiao, A. N. Slavin, and I. N. Krivorotov, Parametric resonance of magnetization excited by electric field, *Nano Lett.* **17**, 572 (2017).
- [27] T. Yamamoto, T. Nozaki, H. Imamura, S. Tamaru, K. Yakushiji, H. Kubota, A. Fukushima, and S. Yuasa, Voltage-driven magnetization switching controlled by microwave electric field pumping, *Nano Lett.* **20**, 6012 (2020).
- [28] H. Imamura and R. Matsumoto, Large-angle precession of magnetization maintained by a microwave voltage, *Phys. Rev. Appl.* **14**, 064062 (2020).
- [29] Y. Shiota, T. Nozaki, F. Bonell, S. Murakami, T. Shinjo, and Y. Suzuki, Induction of coherent magnetization switching in a few atomic layers of FeCo using voltage pulses, *Nat. Mater.* **11**, 39 (2012).
- [30] S. Kanai, M. Yamanouchi, S. Ikeda, Y. Nakatani, F. Matsukura, and H. Ohno, Electric field-induced magnetization reversal in a perpendicular-anisotropy CoFeB-MgO magnetic tunnel junction, *Appl. Phys. Lett.* **101**, 122403 (2012).
- [31] T. Yamamoto, R. Matsumoto, T. Nozaki, H. Imamura, and S. Yuasa, Developments in voltage-controlled subnanosecond magnetization switching, *J. Magn. Magn. Mater.* **560**, 169637 (2022).
- [32] T. Yamamoto, T. Nozaki, H. Imamura, Y. Shiota, T. Ikeura, S. Tamaru, K. Yakushiji, H. Kubota, A. Fukushima, Y. Suzuki, and S. Yuasa, Write-error reduction of voltage-torque-driven magnetization switching by a controlled voltage pulse, *Phys. Rev. Appl.* **11**, 014013 (2019).
- [33] T. Yamamoto, T. Nozaki, H. Imamura, Y. Shiota, S. Tamaru, K. Yakushiji, H. Kubota, A. Fukushima, Y. Suzuki, and S. Yuasa, Improvement of write error rate in voltage-driven magnetization switching, *J. Phys. D: Appl. Phys.* **52**, 164001 (2019).
- [34] W. F. Brown, Thermal fluctuations of a single-domain particle, *Phys. Rev.* **130**, 1677 (1963).
- [35] M. A. W. Schoen, D. Thonig, M. L. Schneider, T. J. Silva, H. T. Nembach, O. Eriksson, O. Karis, and J. M. Shaw, Ultra-low magnetic damping of a metallic ferromagnet, *Nat. Phys.* **12**, 839 (2016).
- [36] S. Mizukami, Y. Ando, and T. Miyazaki, The study on ferromagnetic resonance linewidth for NM/80NiFe/NM (NM = Cu, Ta, Pd and Pt) films, *Jpn. J. Appl. Phys.* **40**, 580 (2001).
- [37] Y. Tserkovnyak, A. Brataas, and G. E. W. Bauer, Enhanced Gilbert damping in thin ferromagnetic films, *Phys. Rev. Lett.* **88**, 117601 (2013).

- [38] S. Mizukami, Y. Ando, and T. Miyazaki, Ferromagnetic resonance linewidth for NM/80NiFe/NM films (NM = Cu, Ta, Pd and Pt), *J. Magn. Magn. Mater.* **1640**, 226 (2001).
- [39] M. Endo, S. Kanai, S. Ikeda, F. Matsukura, and H. Ohno, Electric-field effects on thickness dependent magnetic anisotropy of sputtered MgO/Co₄₀Fe₄₀B₂₀/Ta structures, *Appl. Phys. Lett.* **96**, 212503 (2010).
- [40] T. Nozaki, A. K. Rachwal, W. Skowroński, V. Zayets, Y. Shiota, S. Tamaru, H. Kubota, A. Fukushima, S. Yuasa, and Y. Suzuki, Large voltage-induced changes in the perpendicular magnetic anisotropy of an MgO-based tunnel junction with an ultrathin Fe layer, *Phys. Rev. Appl.* **5**, 044006 (2016).
- [41] Q. Xiang, X. Wen, H. Sukegawa, S. Kasai, T. Seki, T. Kubota, K. Takanashi, and S. Mitani, Nonlinear electric field effect on perpendicular magnetic anisotropy in Fe/MgO interfaces, *J. Phys. D: Appl. Phys.* **50**, 40LT04 (2017).
- [42] A.-K. Rachwał, T. Nozaki, K. Freindl, J. Korecki, S. Yuasa, and Y. Suzuki, Enhancement of perpendicular magnetic anisotropy and its electric field-induced change through interface engineering in Cr/Fe/MgO, *Sci. Rep.* **7**, 5993 (2017).
- [43] T. Yamamoto, T. Nozaki, K. Yakushiji, S. Tamaru, H. Kubota, A. Fukushima, and S. Yuasa, Perpendicular magnetic anisotropy and its voltage control in MgO/CoFeB/MgO junctions with atomically thin Ta adhesion layers, *Acta Mater.* **216**, 117097 (2021).
- [44] X. Li, K. Fitzell, D. Wu, C. T. Karaba, A. Buditama, G. Yu, K. L. Wong, N. Altieri, C. Grezes, N. Kioussis, S. Tolbert, Z. Zhang, J. P. Chang, P. K. Amiri, and K. L. Wang, Enhancement of voltage-controlled magnetic anisotropy through precise control of Mg insertion thickness at CoFeB|MgO interface, *Appl. Phys. Lett.* **110**, 052401 (2017).
- [45] T. Nozaki, M. Endo, M. Tsujikawa, T. Yamamoto, T. Nozaki, M. Konoto, H. Ohmori, Y. Higo, H. Kubota, A. Fukushima, M. Hosomi, M. Shirai, Y. Suzuki, and S. Yuasa, Voltage-controlled magnetic anisotropy in an ultrathin Ir-doped Fe layer with a CoFe termination layer, *APL Mater.* **8**, 011108 (2020).
- [46] S. Miwa, J. Fujimoto, P. Risius, K. Nawaoka, M. Goto, and Y. Suzuki, Strong bias effect on voltage-driven torque at epitaxial Fe-MgO interface, *Phys. Rev. X* **7**, 031018 (2017).
- [47] Z. Wen, H. Sukegawa, T. Seki, T. Kubota, K. Takanashi, and S. Mitani, Voltage control of magnetic anisotropy in epitaxial Ru/Co₂FeAl/MgO heterostructures, *Sci. Rep.* **7**, 45026 (2017).
- [48] A. K. Shukla, M. Goto, X. Xu, K. Nawaoka, J. Suwardy, T. Ohkubo, K. Hono, S. Miwa, and Y. Suzuki, Voltage-controlled magnetic anisotropy in Fe_{1-x}Co_x/Pd/MgO system, *Sci. Rep.* **8**, 10362 (2018).
- [49] W. Skowroński, T. Nozaki, Y. Shiota, S. Tamaru, K. Yakushiji, H. Kubota, A. Fukushima, S. Yuasa, and Y. Suzuki, Perpendicular magnetic anisotropy of Ir/CoFeB/MgO trilayer system tuned by electric fields, *Appl. Phys. Express* **8**, 053003 (2015).
- [50] X. Li, T. Sasaki, C. Grezes, D. Wu, K. Wong, C. Bi, P.-V. Ong, F. Ebrahimi, G. Yu, N. Kioussis, W. Wang, T. Ohkubo, P. K. Amiri, and K. L. Wang, Predictive materials design of magnetic random-access memory based on nanoscale atomic structure and element distribution, *Nano Lett.* **19**, 8621 (2019).
- [51] M. Konoto, H. Imamura, T. Taniguchi, K. Yakushiji, H. Kubota, A. Fukushima, K. Ando, and S. Yuasa, Effect of MgO cap layer on Gilbert damping of FeB electrode layer in MgO-based magnetic tunnel junctions, *Appl. Phys. Express* **6**, 073002 (2013).
- [52] T. Yamamoto, T. Nozaki, Y. Shiota, H. Imamura, S. Tamaru, K. Yakushiji, H. Kubota, A. Fukushima, Y. Suzuki, and S. Yuasa, Thermally induced precession-orbit transition of magnetization in voltage-driven magnetization switching, *Phys. Rev. Appl.* **10**, 024004 (2018).
- [53] T. Ichinose, T. Yamamoto, T. Nozaki, K. Yakushiji, S. Tamaru, and S. Yuasa, Interfacial Fe segregation and its influence on magnetic properties of CoFeB/MgFeO multilayers, *Appl. Phys. Express* **16**, 113002 (2023).
- [54] Y. Shao, V. L.-Dominguez, N. Davila, Q. Sun, N. Kioussis, J. A. Katine, and P. K. Amiri, Sub-volt switching of nanoscale voltage-controlled perpendicular magnetic tunnel junctions, *Commun. Mater.* **87**, 3 (2022).
- [55] T. Ichinose, T. Yamamoto, T. Nozaki, K. Yakushiji, S. Tamaru, M. Konoto, and S. Yuasa, Cryogenic temperature deposition of high-performance CoFeB/MgO/CoFeB magnetic tunnel junctions on ϕ 300 mm wafers, *ACS Appl. Electron. Mater.* **5**, 2178 (2023).
- [56] A. Sugihara, T. Ichinose, S. Tamaru, T. Yamamoto, M. Konoto, T. Nozaki, and S. Yuasa, Low magnetic damping in an ultrathin CoFeB layer deposited on a 300 mm diameter wafer at cryogenic temperature, *Appl. Phys. Express* **16**, 023003 (2023).
- [57] S. Tamaru, T. Yamamoto, T. Onuma, N. Kikuchi, and S. Okamoto, Development of a high-sensitivity VNA-FMR spectrometer with field modulation detection and its application to magnetic characterization, *Electron. Commun. Jpn.* **104**, e12320 (2021).
- [58] S. Tamaru, T. Yamamoto, T. Nozaki, and S. Yuasa, Accurate calculation and shaping of the voltage pulse waveform applied to a voltage-controlled magnetic random access memory cell, *Jpn. J. Appl. Phys.* **57**, 073002 (2018).